INTERNATIONAL JOURNAL FOR NUMERICAL METHODS IN ENGINEERING
Int. J. Numer. Meth. Engng 2003; **57**:835–851 (DOI: 10.1002/nme.707)

Symmetric-Galerkin BEM simulation of fracture with frictional contact

A.-V. Phan[1,*,†], J. A. L. Napier[2], L. J. Gray[3] and T. Kaplan[3]

[1]*Department of Mechanical Engineering, University of South Alabama, Mobile, AL 36688-0002, U.S.A.*
[2]*CSIR, Division of Mining Technology, Auckland Park 2006, Johannesburg, South Africa*
[3]*Computer Science and Mathematics Division, Oak Ridge National Laboratory, Oak Ridge, TN 37831-6367, U.S.A.*

SUMMARY

A symmetric-Galerkin boundary element framework for fracture analysis with frictional contact (crack friction) on the crack surfaces is presented. The algorithm employs a *continuous* interpolation on the crack surface (utilizing quadratic boundary elements) and enables the determination of two important quantities for the problem, namely the local normal tractions and sliding displacements on the crack surfaces. An effective iterative scheme for solving this non-linear boundary value problem is proposed. The results of test examples are compared with available analytical solutions or with those obtained from the displacement discontinuity method (DDM) using linear elements and internal collocation. The results demonstrate that the method works well for difficult kinked/junction crack problems. Copyright © 2003 John Wiley & Sons, Ltd.

KEY WORDS: crack friction; fracture analysis; kinked crack; boundary element method; symmetric-Galerkin approximation

1. INTRODUCTION

The two principal approaches for computational fracture analysis are the finite element method (FEM) (e.g. Reference [1]) and boundary element method (BEM) [2–5]. The key feature of the integral equation approach is that only the boundary of the domain is discretized and only boundary quantities are determined. As a result, the singular stress field ahead of the crack is not approximated in the analysis, and moreover, remeshing a propagating crack is easier. In this regard, it should be noted that automatic volume meshing routines are now available

*Correspondence to: A.-V. Phan, Department of Mechanical Engineering, University of South Alabama, Mobile, AL 36688-0002, U.S.A.
†E-mail: vphan@jaguarl.usouthal.edu

Contract/grant sponsor: U.S. Department of Energy; contract/grant number: DE-AC05-00 OR22725
Contract/grant sponsor: UT-Battelle, LLC

Received 17 December 2001
Revised 5 August 2002
Accepted 6 September 2002

[6] and that recent finite element work on meshless [7] and eXtended FEM (X-FEM) [8, 9] methods avoid explicit remeshing of the crack.

Contact friction boundary conditions arise in problems relating to rolling and sliding between machine components or other bodies [10–12] and are ubiquitous in the fields of earthquake science, rock mechanics and geotechnical engineering, where multiple interacting faults and discontinuities are present. The numerical treatment of these problems often presents a number of difficulties in that boundary conditions are specified in the form of inequality constraints rather than in terms of fixed tractions or displacements. Further difficulties arise when multiple intersecting junctions are considered in a cracked material (kinked crack problems). For two-dimensional (2D) problems, a rosette of interacting wedge structures have to be analysed with, in general, power-law displacement functions on each wedge face. Three-dimensional junctions are correspondingly more demanding. In the face of this complexity it is clear that purely analytic approaches will be severely restricted. However, as the deformation field in the vicinity of a junction point may be non-analytic, it is essential to have confidence in any proposed numerical procedure that may rely on a limited representation of the deformation shape solution.

Thus far, FEM [13], BEM using an integral equation for the resultant forces along a crack [14–16], multi-domain BEM [17], dual BEM [18] and displacement discontinuity method (DDM) [19–22] are numerical methods that have been employed for crack friction problems. Note that DDM is a BEM technique based on the analytical solution to the problem of a constant discontinuity in displacement over a single crack in unbounded domain. All these BEM techniques are collocation methods as they employ collocation at either boundary nodes or internal nodes (internal collocation).

The goal of this work is to demonstrate that the symmetric-Galerkin boundary element method (SGBEM) [23–25] provides accurate solutions for crack friction problems, and more specifically, for kinked and junction fractures. Frictional contact results using symmetric-Galerkin for smooth cracks have been previously reported in Reference [26]. Symmetric-Galerkin employs a Galerkin approximation of both the standard displacement integral equation and the hypersingular traction equation, with this latter equation being enforced on the crack surface [27–29]. As with most DDM implementations, the crack opening displacement (COD) is employed as the unknown quantity on the crack surface. The Galerkin procedure is based upon an additional boundary integration, and is thus potentially more time consuming than collocation. However, the extra computational expense can be partially offset by exploiting symmetry, both in the matrix construction phase [30] and in solving the linear system. Note too that internal collocation requires many more unknowns (for the same discretization), and thus Galerkin is in fact likely to be more efficient, especially in three dimensions. Equally important, two key advantages follow from the Galerkin procedure. First, unlike collocation, there is no smoothness requirement on the displacement [31, 32] in order to evaluate the hypersingular integral; thus, standard *continuous* elements can be employed. The Galerkin approach can therefore easily exploit the highly effective quarter point quadratic element to accurately capture the crack tip behaviour. Internal collocation on the other hand results in a physically unappealing *discontinuous* interpolation. Second, the weighted averaging formulation of Galerkin, by avoiding direct collocation at corners and junction points, provides a smoother solution in the neighbourhood of geometric discontinuities. This is especially useful for the kinked crack problems considered herein.

This paper is organized as follows. In the next section, a review of the SGBEM for fracture mechanics is given. Section 3 briefly describes the DDM with internal collocation. In Section 4, an algorithm using the SGBEM for solving crack friction problems is presented. In Section 5, several numerical examples are solved and are compared with reference solutions. The last section contains some concluding remarks.

2. SYMMETRIC-GALERKIN BOUNDARY INTEGRAL FORMULATION

This section provides a very brief review of boundary integral equations for elasticity, and their approximation via the symmetric-Galerkin procedure. The reader is asked to consult the cited references for further details.

The boundary integral equation (BIE) without body forces for linear elasticity is given by Rizzo [33]. For a source point P interior to the domain, this equation takes the form

$$u_k(P) - \int_{\Gamma_b} [U_{kj}(P,Q)\tau_j(Q) - T_{kj}(P,Q)u_j(Q)]\,\mathrm{d}Q = 0 \tag{1}$$

where Q is a field point, τ_j and u_j are traction and displacement vectors, U_{kj} and T_{kj} are the Kelvin kernel tensors or fundamental solutions, Γ_b denotes the boundary of the domain, and $\mathrm{d}Q$ is an infinitesimal boundary length (for 2D) or boundary surface (for 3D cases).

For plane strain problems (see, e.g. Reference [33]),

$$U_{kj} = \frac{1}{8\pi G(1-\nu)}[r_{,k}r_{,j} - (3-4\nu)\delta_{kj}\ln(r)] \tag{2}$$

$$T_{kj} = -\frac{1}{4\pi(1-\nu)r}\left[\{(1-2\nu)\delta_{kj} + 2r_{,k}r_{,j}\}\frac{\partial r}{\partial n} - (1-2\nu)(n_j r_{,k} - n_k r_{,j})\right] \tag{3}$$

where ν is Poisson's ratio, G is shear modulus, δ_{ij} is the Kronecker delta ($\equiv 1$ for $i=j$ and $\equiv 0$ for $i\neq j$), $r_k = x_k(Q) - x_k(P)$, $r^2 = r_i r_i$, $r_{,k} = r_k/r$ and $\partial r/\partial n = r_{,i}n_i$.

It can be shown that the limit of the integral in Equation (1) as P approaches the boundary exists. From now on, for $P\in\Gamma_b$, the BIE is understood in this limiting sense.

As P is off the boundary, the kernel functions are not singular and it is permissible to differentiate Equation (1) with respect to P, yielding the hypersingular BIE (HBIE) for displacement gradient. Substitution of this gradient into Hooke's law gives the following HBIE for boundary stresses:

$$\sigma_{k\ell}(P) - \int_{\Gamma_b} [D_{kj\ell}(P,Q)\tau_j(Q) - S_{kj\ell}(P,Q)u_j(Q)]\,\mathrm{d}Q = 0 \tag{4}$$

where

$$D_{kj\ell} = \frac{1}{4\pi(1-\nu)r}[(1-2\nu)(\delta_{kj}r_{,\ell} + \delta_{j\ell}r_{,k} - \delta_{\ell k}r_{,j}) + 2r_{,k}r_{,j}r_{,\ell}] \tag{5}$$

$$\begin{aligned} S_{kj\ell} = \frac{G}{2\pi(1-\nu)r^2}\Bigg[&2\frac{\partial r}{\partial n}\{(1-2\nu)\delta_{\ell k}r_{,j} + \nu(\delta_{kj}r_{,\ell} + \delta_{j\ell}r_{,k}) - 4r_{,k}r_{,j}r_{,\ell}\} \\ &+ 2\nu(n_k r_{,j}r_{,\ell} + n_\ell r_{,k}r_{,j}) + (1-2\nu)(2n_j r_{,\ell}r_{,k} + \delta_{kj}n_\ell + \delta_{j\ell}n_k) - (1-4\nu)\delta_{\ell k}n_j\Bigg] \end{aligned} \tag{6}$$

The Galerkin boundary integral formulation is obtained by taking the shape functions ψ_m employed in approximating the boundary tractions and displacements as weighting functions for the integral equations (1) and (4). Thus,

$$\int_{\Gamma_b} \psi_m(P) u_k(P)\,\mathrm{d}P - \int_{\Gamma_b} \psi_m(P) \int_{\Gamma_b} [U_{kj}(P,Q)\tau_j(Q) - T_{kj}(P,Q)u_j(Q)]\,\mathrm{d}Q\,\mathrm{d}P = 0 \quad (7)$$

$$\int_{\Gamma_b} \psi_m(P) \sigma_{k\ell}(P)\,\mathrm{d}P - \int_{\Gamma_b} \psi_m(P) \int_{\Gamma_b} [D_{kj\ell}(P,Q)\tau_j(Q) - S_{kj\ell}(P,Q)u_j(Q)]\,\mathrm{d}Q\,\mathrm{d}P = 0 \quad (8)$$

A symmetric coefficient matrix, and hence a symmetric-Galerkin approximation, is obtained by employing Equation (7) on the boundary $\Gamma_{b(\mathbf{u})}$ where displacements u_{bv} are prescribed, and similarly using Equation (8) is employed on the boundary $\Gamma_{b(\tau)}$ with prescribed tractions τ_{bv}. Note that $\Gamma_b = \Gamma_{b(\mathbf{u})} + \Gamma_{b(\tau)}$.

A solution procedure that employs a collocation approach enforces the BIE (1) and HBIE (4) at discrete source points whereas these equations are satisfied in an averaged sense with the Galerkin approximation. The additional boundary integration is the key to obtaining a symmetric coefficient matrix, as this ensures that the source point P and field point Q are treated in the same manner in evaluating the kernel tensors U_{kj}, T_{kj}, $D_{kj\ell}$ and $S_{kj\ell}$. After discretization, the resulting equation system can be written as

$$\begin{bmatrix} H_{11} & H_{12} \\ H_{21} & H_{22} \end{bmatrix} \begin{Bmatrix} u_{bv} \\ u_* \end{Bmatrix} = \begin{bmatrix} G_{11} & G_{12} \\ G_{21} & G_{22} \end{bmatrix} \begin{Bmatrix} \tau_* \\ \tau_{bv} \end{Bmatrix} \quad (9)$$

Here, the first and second rows represent, respectively, the BIE written on $(\Gamma_{b(\mathbf{u})})$ and the HBIE on $(\Gamma_{b(\tau)})$. Further, u_* and τ_* denote unknown displacement and traction vectors. Rearranging Equation (9) into the form $[A]\{x\} = \{b\}$, and multiplying the HBIE by -1, one obtains

$$\begin{bmatrix} -G_{11} & H_{12} \\ G_{21} & -H_{22} \end{bmatrix} \begin{Bmatrix} \tau_* \\ u_* \end{Bmatrix} = \begin{Bmatrix} -H_{11}u_{bv} + G_{12}\tau_{bv} \\ H_{21}u_{bv} - G_{22}\tau_{bv} \end{Bmatrix} \quad (10)$$

The symmetry of the coefficient matrix, $G_{11} = G_{11}^{\mathrm{T}}$, $H_{22} = H_{22}^{\mathrm{T}}$ and $H_{12} = G_{21}^{\mathrm{T}}$ now follows from the symmetry properties of the kernel tensors.

2.1. Cracks in finite domains

A finite domain or body, B, of general shape is shown in Figure 1. The body is shown to include a crack surface denoted as Γ_c on which only tractions are prescribed. Initially, the crack is composed of two coincident surfaces according to $\Gamma_c = \Gamma_c^+ + \Gamma_c^-$ where Γ_c^+ and Γ_c^- denote the upper and lower crack surfaces, respectively. As a result, the outward normals to the crack surfaces, $\mathbf{n}_c^+$ and $\mathbf{n}_c^-$, are oriented oppositely so that $\mathbf{n}_c^- = -\mathbf{n}_c^+$. Thus, the BIE and

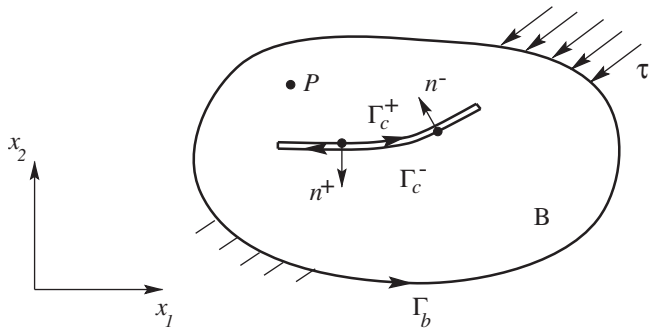

Figure 1. A body B containing a fracture.

HBIE written for an interior point P then take the following forms:

$$u_k(P) = \int_{\Gamma_b} [U_{kj}(P,Q)\tau_j(Q) - T_{kj}(P,Q)u_j(Q)]\,\mathrm{d}Q + \int_{\Gamma_c^+} [U_{kj}(P,Q)\Sigma\tau_j(Q) - T_{kj}(P,Q)\Delta u_j(Q)]\,\mathrm{d}Q \tag{11}$$

$$\sigma_{k\ell}(P) = \int_{\Gamma_b} [D_{\ell km}(P,Q)\tau_m(Q) - S_{\ell km}(P,Q)u_m(Q)]\,\mathrm{d}Q + \int_{\Gamma_c^+} [D_{\ell km}(P,Q)\Sigma\tau_m(Q) - S_{\ell km}(P,Q)\Delta u_m(Q)]\,\mathrm{d}Q \tag{12}$$

where, only the upper crack surface Γ_c^+ needs to be modelled as on the two crack surfaces, the displacements $\mathbf{u}_c^+$ and $\mathbf{u}_c^-$ are replaced by the single COD $\Delta\mathbf{u}_c = \mathbf{u}_c^+ - \mathbf{u}_c^-$, and the tractions $\boldsymbol{\tau}_c^+$ and $\boldsymbol{\tau}_c^-$ by the sum of tractions $\Sigma\boldsymbol{\tau}_c = \boldsymbol{\tau}_c^+ + \boldsymbol{\tau}_c^-$. However, since the crack surfaces are usually symmetrically loaded, i.e. $\boldsymbol{\tau}_c^- = -\boldsymbol{\tau}_c^+$, one gets

$$u_k(P) = \int_{\Gamma_b} [U_{kj}(P,Q)\tau_j(Q) - T_{kj}(P,Q)u_j(Q)]\,\mathrm{d}Q - \int_{\Gamma_c^+} T_{kj}(P,Q)\Delta u_j(Q)\,\mathrm{d}Q \tag{13}$$

$$\sigma_{k\ell}(P) = \int_{\Gamma_b} [D_{\ell km}(P,Q)\tau_m(Q) - S_{\ell km}(P,Q)u_m(Q)]\,\mathrm{d}Q - \int_{\Gamma_c^+} S_{\ell km}(P,Q)\Delta u_m(Q)\,\mathrm{d}Q \tag{14}$$

It can be shown that a symmetric coefficient matrix can be achieved by using $\Delta\mathbf{u}$ as variables on Γ_c^+. Following the Galerkin approximation, the limit of (13) and (14) is taken as $P \to \Gamma_{b(\mathbf{u})}$ and $\Gamma_{b(\boldsymbol{\tau})}$, respectively. At this point, it is convenient to convert the stress equation (14) into a traction equation through the identity $\tau_k(P) = \sigma_{\ell k}(P)n_\ell(P)$, with $n_\ell(P)$ being the outward normal at P. After discretizing, the following system established from Equations (13)

and (14) is obtained:

$$[G_{bb}]\{\tau_b\} = [H_{bb}]\{u_b\} + [H_{bc}]\{\Delta u_c\} \tag{15}$$

where b and c denote the outer boundary and upper crack surface, respectively.

Since tractions are prescribed on the crack, only Equation (14) is written for source points on Γ_c^+. Again, following the Galerkin approximation, the limit of (14) as $P \to \Gamma_c$, the conversion of (14) into a traction equation, and discretization, the result is

$$[G_{cb}]\{\tau_b\} - [G_{cc}]\{\tau_c^+\} = [H_{cb}]\{u_b\} + [H_{cc}]\{\Delta u_c\} \tag{16}$$

Note that $\boldsymbol{\tau}_c^+$ now appears on the left-hand side of Equation (16) due to the limit process as $P \to \Gamma_c$. Combining Equations (15) and (16), the equation system of the problem can be written as follows:

$$\begin{bmatrix} H_{bb} & H_{bc} \\ H_{cb} & H_{cc} \end{bmatrix} \begin{Bmatrix} u_b \\ \Delta u_c \end{Bmatrix} = \begin{bmatrix} G_{bb} & 0 \\ G_{cb} & G_{cc} \end{bmatrix} \begin{Bmatrix} \tau_b \\ -\tau_c^+ \end{Bmatrix} \tag{17}$$

where it can be proved that the coefficient matrix on the left-hand side of (17) is also symmetric.

2.2. *Cracks in unbounded domains*

When an unbounded domain is considered and is subjected to uniform remote stress $\bar{\sigma}_{ij}$, Equation (16) reduces to the following system:

$$-[G_{cc}]\{\tau_c^+\} = [H_{cc}]\{\Delta u_c\} \tag{18}$$

where $\{\tau_c^+\}$ on the upper crack surface Γ_c^+ is now the superposition of the prescribed tractions directly applied on Γ_c^+ and the tractions $\bar{\sigma}_{ij} n_j^+$ due to the remote stresses $\bar{\sigma}_{ij}$. Note that n_j^+ are the components of the outward normal $\mathbf{n}_c^+$ to Γ_c^+.

2.3. *Interpolation using quadratic elements*

In 2D, the representation of a quantity $V(t)$ (geometry, displacement, traction,...) using the three-equidistant-noded quadratic element (or standard quadratic element) is

$$V_k(t) = \sum_{j=1}^{3} V_{kj} \psi_j(t) \tag{19}$$

where V_{kj} are the nodal values of V_k, and the shape functions $\psi_j(t)$ for $0 \leqslant t \leqslant 1$ are given by

$$\begin{aligned} \psi_1(t) &= (1-t)(1-2t) \\ \psi_2(t) &= 4t(1-t) \\ \psi_3(t) &= t(2t-1) \end{aligned} \tag{20}$$

In crack analysis, the COD can also be interpolated using Equations (19) and (20). However, a quarter-point element needs to be associated with each crack tip in order to account

for the stress singularity and the $\sqrt{r}$ behaviour at the crack tip, where r is the distance from a source point to the tip [34, 35]. The quarter-point element is formed from the standard quadratic element by simply moving the mid-node co-ordinates three-fourths of the way towards the tip.

Recently, a modified quarter-point element was proposed [36] and the SGBEM calculations reported in this paper use this element. It was shown that the accuracy of the crack tip stress intensity factors can be significantly improved by using the modified quarter-point element. This would be important if crack propagation in these systems was being investigated.

3. DDM FORMULATION WITH INTERNAL COLLOCATION

Analytical solutions for geometrically complex crack friction problems are rare, so it is necessary to validate the SG results using alternative numerical solutions. In this paper, the DDM approximation based upon internal collocation will be used for this purpose. We therefore present a brief description of this approach.

As indicated in the previous section, traditional boundary element solution procedures follow a formulation in which the characteristic boundaries of the problem region are tessellated by a contiguous covering of surface patches or line segments termed 'elements'. A straightforward solution procedure can be implemented if no continuity requirements are imposed on the unknown surface variables at the junctions between adjacent elements (so-called 'non-conforming' approximation [37]). In this case, the local variation of the unknown surface quantities can be described by shape functions whose nodal points fall within the element boundaries at specified internal collocation points. As a simple example, consider a straight-line element in which any position within the element is defined by an intrinsic variable t having range $-1 \leqslant t \leqslant 1$. If a linear variation of the unknown variables is assumed, it is necessary to define two collocation points at positions $t = \pm c$ within the element where $0 < c < 1$. The corresponding shape functions are defined to be

$$\begin{aligned} \psi_1(t) &= \frac{1}{2}\left(1 - \frac{t}{c}\right); \quad -1 \leqslant t \leqslant 1 \\ \psi_2(t) &= \frac{1}{2}\left(1 + \frac{t}{c}\right); \quad -1 \leqslant t \leqslant 1 \end{aligned} \tag{21}$$

The variation of a given quantity over the element is expressed as

$$V(t) = V_1\psi_1(t) + V_2\psi_2(t) \tag{22}$$

where V_1 and V_2 are the values defined at each collocation point. The advantage of this approach is that displacement and traction vectors can be evaluated analytically at the internal collocation point positions where the boundary surface is locally smooth.

In the solution of a contact friction problem using this formulation, the local traction vector $\boldsymbol{\tau}$ at collocation position P can be expressed in the form

$$\boldsymbol{\tau}(P) = \mathbf{K}\mathbf{u}(P) + \mathbf{e}(P) + \mathbf{f}(P) \tag{23}$$

where $\mathbf{K}$ is the self-effect influence matrix, $\mathbf{u}(P)$ is the unknown surface displacement (or displacement discontinuity) vector associated with collocation point P, $\mathbf{e}(P)$ is the sum of all tractions induced at point P by all collocation positions other than point P and $\mathbf{f}(P)$ is the initial field stress at point P. The solution of a system of equations for the unknown vectors $\mathbf{u}(P)$ can be carried out conveniently using an iterative procedure. Details of this approach are described in Reference [21]. The main utility of this scheme is that general non-linear constraints can be imposed at each collocation point. In particular, constraints between shear and normal components of the traction vector $\boldsymbol{\tau}$, imposed by sliding friction or by non-linear joint stiffness relationships can be easily resolved. On the other hand, two major disadvantages are associated with the internal collocation scheme. Firstly, the relaxation of continuity requirements at element boundaries and junctions will lead to singularities in the stress field in the vicinity of these points. If multiple, closely spaced crack assemblies are to be analysed, this can, in certain cases, lead to numerical difficulties. A second disadvantage is that the internal collocation scheme is inherently less efficient than approaches such as the symmetric-Galerkin procedure described in this paper, in which the unknown solution variables can be specified at both the element junctions and at internal element positions. For example, in a 2D crack problem comprising n elements, the number of internal collocation points required is $3n$ if quadratic variation shape functions are employed. In the symmetric-Galerkin scheme, the number of nodal points would be $(2n-1)$. The reduction in nodal positions is correspondingly greater when three-dimensional surfaces are considered.

4. CRACK FRICTION ALGORITHM USING THE SGBEM

In this section, we present a framework to model cracks with frictional contact using the SGBEM. This is a non-linear boundary value problem which can be resolved by adopting an iterative scheme. This scheme enables the determination of two important quantities, namely the normal tractions and sliding displacements (slip) on the sliding crack surfaces. In the following sections, it is shown that the symmetric-Galerkin procedure can also be formulated to resolve problems of friction sliding in cases where the friction constraint condition may be different on each branch of a common junction point.

4.1. Problem formulation

Consider a body B (or an unbounded domain) containing internal cracks subjected to prescribed global tractions $\boldsymbol{\tau}_c$. Let Δu_n and Δu_t be, respectively, the crack opening/closing and sliding displacements in the local co-ordinate system (t,n). After the final solution of the iterative scheme is converged, additional local tractions $\mathbf{t}=(t_t,t_n)$ on the sliding crack surfaces are determined such that no material interpenetration occurs. Note that t_n and t_t are, respectively, the normal and tangential components of $\mathbf{t}$. The boundary conditions for the final solution are:

1. Either $\Delta u_n=0$ and $\Delta u_t=0$ (the crack is not sliding), in which case $\mathbf{t}=0$, or
2. $\Delta u_n>0$ (the crack is open), also in which case $\mathbf{t}=0$, or
3. Δu_n is forced to be 0 (no material interpenetration, the crack is sliding) by applying additional tractions $\mathbf{t}$ on those crack surfaces; the normal and tangential components of $\mathbf{t}$ are related by $|t_t|=-\tan(\phi)t_n$ with ϕ being the friction angle. The sign of t_t is such that the sliding movement of the crack surfaces is opposed.

Note that t_n is non-linearly dependent on the Δu_n values on all other cracks and on the field stress.

4.2. Iterative procedure

For crack friction problems, the numerical solution with the initial traction boundary conditions on the crack surfaces provides negative Δu_n (material interpenetration) in the region of contact. This negative Δu_n solution is obviously unphysical, and thus an iterative procedure is employed to determine t_n and t_t such that $\Delta u_n \geqslant 0$:

1. From the SGBEM solution for the global COD $\Delta \mathbf{u}_c$, compute the local displacement components Δu_n and Δu_t.
2. If $\Delta u_n < 0$ at a given node on the crack, set:
   (a) Normal traction at the ith step as $t_n^{(i)} = t_n^{(i-1)} - k\Delta u_n$, where $t_n^{(i-1)}$ is the normal traction at the previous step, and $k = G/b$ with G and b being the shear modulus and crack length, respectively,
   (b) $t_t = \text{sign}(\Delta u_t) \tan(\phi) t_n$.
3. At the crack tips of a sliding crack, normal tractions $t_n^{(i)}$ are determined by interpolating those at the other nodes of the crack tip elements.
4. Convert the local traction components t_n and t_t to the global traction vector $\boldsymbol{\tau}_{ca}^{+}$ on the upper crack surface.
5. Superpose the above additional tractions $\boldsymbol{\tau}_{ca}^{+}$ to the initially prescribed tractions $\boldsymbol{\tau}_c^{+}$ on the crack surface. Re-solve the SGBEM system (17).
6. Repeat from the first step until convergence.

The error indicator of convergence is calculated after each iterative step as the maximum difference between the current and previous computed local normal traction component

$$\varepsilon = \max |t_n^{(i)} - t_n^{(i-1)}| \tag{24}$$

The iteration process is converged when the error indicator ε is below a specified tolerance ε_0.

5. TEST CASES

Four problems are reported in this section to illustrate the proposed algorithm using the SGBEM. Unless otherwise noted, the plane strain state is considered, the material constants employed are Young's modulus $E = 70\,000$ MPa and Poisson's ratio $v = 0.2$, and a convergence criterion $\varepsilon_0 = 10^{-6}$ MPa is chosen.

5.1. Single crack under compression

A single crack in an unbounded domain and subject to a compressive remote stress $\sigma = 200$ MPa (see Figure 2) is studied first, as an analytical solution is available for comparison. The crack length and inclination angle are $2b = 10$ m and $\alpha = 20°$, respectively. A friction angle $\phi = 30°$ is assumed.

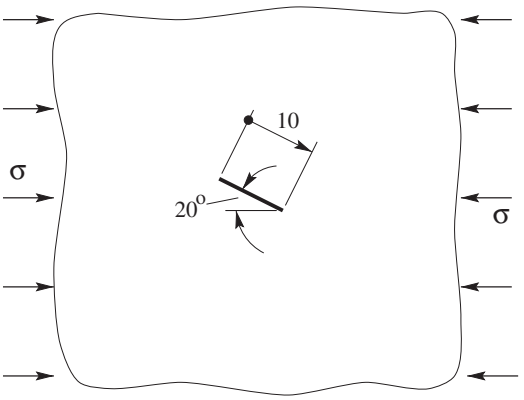

Figure 2. A crack under compression in an unbounded domain.

The analytical solutions for the normal traction t_n and slip Δu_t on the crack surface are given by

$$t_n = -\sigma \sin^2 \alpha \tag{25}$$

$$\Delta u_t = \frac{4(1-\nu^2)\tau_t^c}{E} \sqrt{b^2 - (\eta - b)^2} \tag{26}$$

where $\sigma < 0$, $0 \leqslant \eta \leqslant 2b$ and the shear traction τ_t^c on the crack surface in the presence of frictional contact is

$$\tau_t^c = \sigma \sin \alpha (\cos \alpha - \sin \alpha \tan \phi) \tag{27}$$

For numerical analysis by the SGBEM, the crack is discretized into ten quadratic elements of equal length. The numerical and analytical solutions for t_n and Δu_t that are plotted in Figure 3 are practically identical.

5.2. Two-wing crack problem

Consider a two-wing crack in an infinite plate under a far-field compressive stress $\sigma = 200$ MPa acting in the plate's plan as depicted in Figure 4. This kinked crack is formed by three segments of equal length. Due to the compressive loading, the surfaces of the inclined crack segment are in contact. The cases of frictionless ($\phi = 0$) and frictional contacts ($\phi = 30°$) are of interest.

For numerical analysis by the SGBEM, 10 and 14 quadratic elements are used to discretize each of the horizontal segments and the inclined segment of the crack, respectively. These are non-uniform elements with shorter ones being placed near the junction points. It is known that the dislocation densities contain a singularity at a crack kink, and the mesh refinement technique can be used to handle this singularity [14]. Numerical analysis carried out by the internal collocation DDM uses ten linear elements to discretize each of the crack segments. The SGBEM and DDM solutions for normal traction t_n and slip Δu_t on the inclined segment of the crack are plotted in Figure 5 for the frictionless case, and in Figure 6 for the frictional

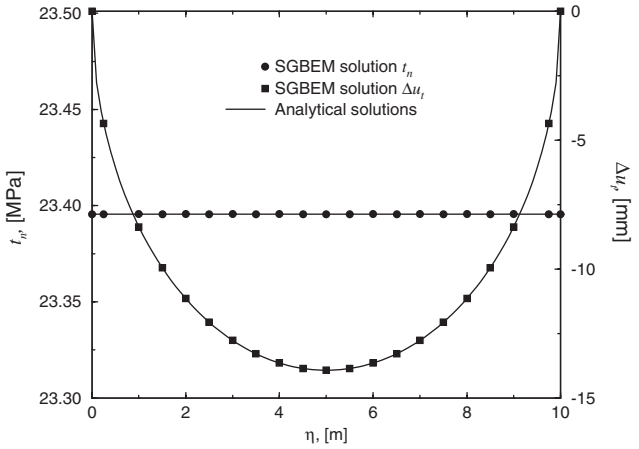

Figure 3. Normal traction and slip on the crack ($\phi = 30°$).

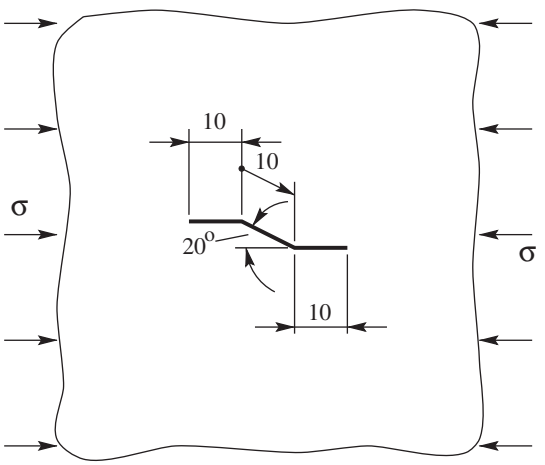

Figure 4. A Two-wing crack in an unbounded domain.

case. Very good agreement between the SGBEM and DDM solutions can be observed. The normal tractions shown in Figure 6 (with friction on the sliding crack) can be seen to be slightly higher than the case with no friction (Figure 5).

5.3. *Crack intersection problem*

This problem arises from attempting to simulate a mining problem. A sliding crack intersecting at right angles to the right-hand edge of a horizontal crack in a bi-axial compressive far-field stress is shown in Figure 7. The traction-free horizontal 'crack' represents an approximation to a slot-shaped opening having a large length to width aspect ratio. Allowing interpenetration is interpreted as the movement of the roof and the floor towards each other when this opening

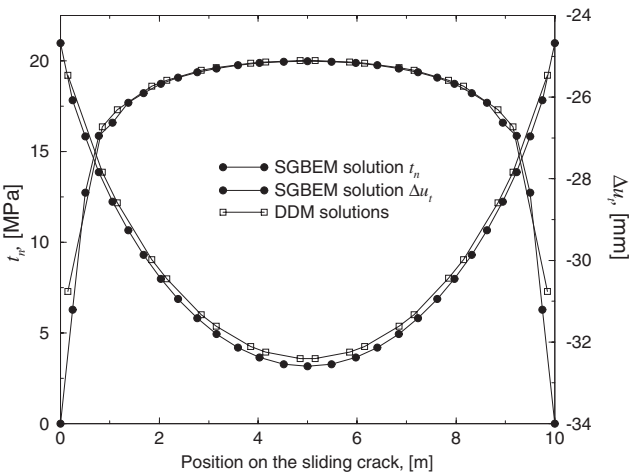

Figure 5. Normal traction and slip on the sliding (inclined) segment of the crack ($\phi = 0$).

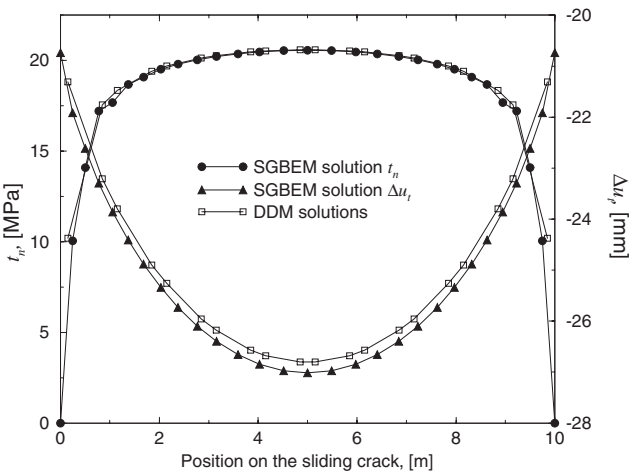

Figure 6. Normal traction and slip on the (sliding) inclined segment of the crack ($\phi = 30^\circ$).

is established in the compressive stress field mentioned above. The vertical crack represents a fault intersecting the end of the opening, and thus its surfaces are not allowed to interpenetrate.

For numerical analyses, $\sigma = 100$ MPa and a frictional angle $\phi = 30^\circ$ are considered. The internal collocation DDM employs 40 uniform linear elements, while the SGBEM uses 20 non-uniform quadratic elements to mesh each of the crack segments. As usual, shorter elements are located near the intersection point. The numerical solutions for local normal traction t_n and slip Δu_t on the fault are depicted in Figure 8. Good agreement between the SGBEM and DDM solutions can be seen.

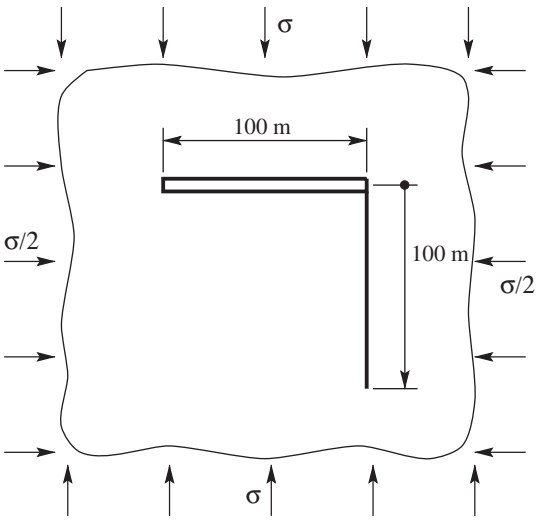

Figure 7. Intersecting cracks in an unbounded domain.

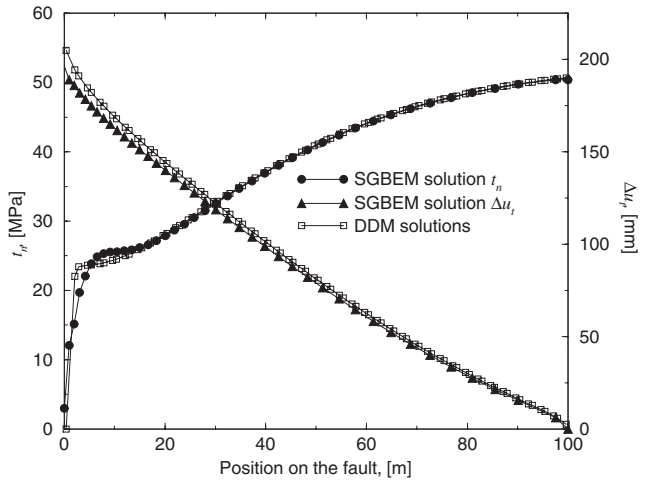

Figure 8. Normal traction and slip on the fault.

5.4. *T-crack problem*

Finally, consider a T-crack in an unbounded domain and subject to a remote compressive stress $\sigma = 100\,\text{MPa}$ acting vertically (see Figure 9). The vertical segment of this kinked crack is horizontally pressurized to $p = 100\,\text{MPa}$ internally and intersects the middle of the horizontal (sliding) crack segment at right angles. A frictional angle $\phi = 30^\circ$ is used.

For the DDM simulation, 200 and 400 uniform elements are employed to discretize the horizontal and vertical cracks, respectively. For the SGBEM simulation, the corresponding

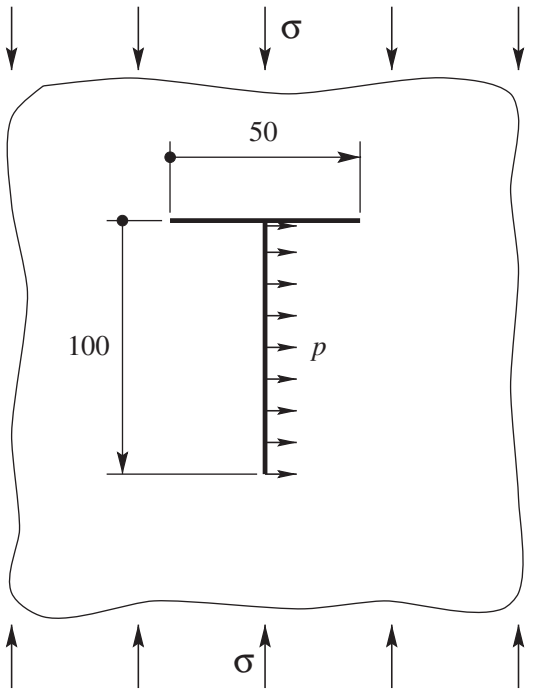

Figure 9. A *T*-crack in an unbounded domain.

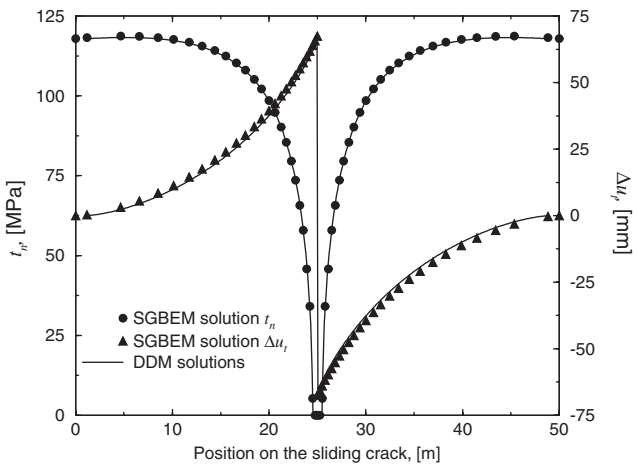

Figure 10. Normal traction and slip on the sliding (horizontal) segment of the crack.

numbers of elements are 26 and 41. Again, shorter SGBEM elements are placed near the junction point. The SGBEM versus DDM solutions for normal pressures t_n and slip Δu_t on the sliding segment of the crack are plotted in Figure 10 where the agreement is very good.

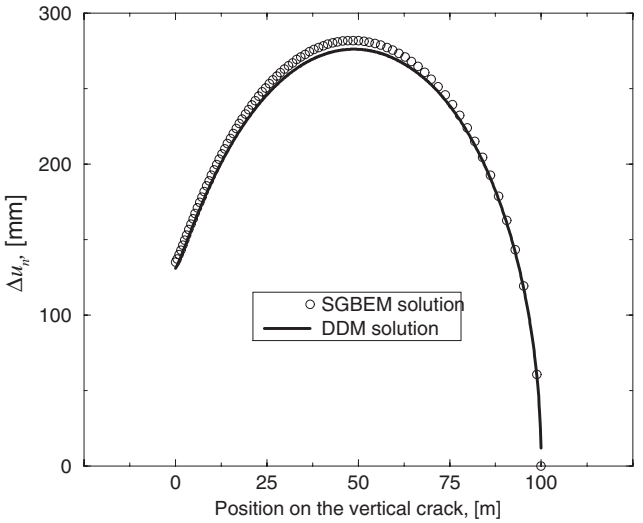

Figure 11. COD on the vertical segment of the crack.

It appears from both the SGBEM and DDM solutions that the sliding crack opens slightly adjacent to the point of intersection with the pressurized crack.

The numerical results for the COD on the vertical crack are shown in Figure 11 where, again, very good agreement is observed. Note that the COD at the intersection point is equal to the jump in the slip on the sliding crack at that point (see Figure 10). While the SGBEM is able to produce the COD at the intersection point (COD = 134.98 mm) and at crack tip (COD = 0), the DDM cannot, as there is no collocation at these points.

6. CONCLUDING REMARKS

An algorithm for modelling crack problems with frictional contact based upon a symmetric-Galerkin analysis has been presented. An iterative scheme is adopted to solve the system of non-linear equations on the crack surface. Two important advantages of the SGBEM are exploited, namely the ability to use standard continuous elements to solve crack problems, and the ability to accurately handle corners and junction points. One consequence of this is that the elegant quarter point element can be employed to accurately capture the crack tip singularity. The results of the test problems, deliberately chosen to examine the behaviour of the algorithm for problems involving kinks and junction points, demonstrate that the approach is very successful. This suggests that the SGBEM is a very effective method for solving problems with crack friction constraints.

In applying the friction interface model, we have specified an inequality constraint that requires the friction resistance on the sliding interface to be greater than or equal to the shear stress acting across the interface. Consequently, the solutions that satisfy this form of boundary condition are not necessarily unique. For example, if one of the existing solutions was considered and a small reverse slip was applied to a section of the sliding interface, then the

inequality could still be satisfied although the 'solution' would be different but still valid in terms of the stated boundary constraint. In addition, we do not treat explicit time-dependent rate/state friction constitutive rules or general time-dependent evolution of the solution. In order to provide a 'sensible engineering' result, satisfying the boundary conditions, it is necessary therefore to consider all loading steps to be suitably 'small' and to be arranged in a defined sequence.

Based upon these encouraging two-dimensional results, future work will examine the extension of the method to three-dimensional crack friction problems. Note that in this higher dimension, internal collocation necessarily requires many more unknowns (due to the non-conforming approximation) than a corresponding SGBEM calculation, and would therefore be highly inefficient. Moreover, crack junctions now become one-dimensional edges (instead of a zero-dimensional point), and thus too would pose a challenge to collocation-based approaches.

ACKNOWLEDGEMENTS

This research was supported in part by the Applied Mathematical Sciences Research Program of the Office of Mathematical, Information, and Computational Sciences, U.S. Department of Energy under contract DE-AC05-00OR22725 with UT-Battelle, LLC.

REFERENCES

1. Cook RD, Malkus DS, Plesha ME. *Concepts and Applications of Finite Element Analysis.* Wiley: New York, 1989.
2. Cruse TA. *Boundary Element Analysis in Computational Fracture Mechanics*. Kluwer Academic Publishers: Boston, 1988,
3. Crouch SL, Starfield AM. *Boundary Element Methods in Solid Mechanics*. Unwin Hyman: London, 1990.
4. Aliabadi MH. Boundary element formulations in fracture mechanics. *Applied Mechanics Reviews* 1997; **50**:83–96.
5. Chen JT, Hong H-K. Review of dual boundary element methods with emphasis on hypersingular integrals and divergent series. *Applied Mechanics Reviews* 1999; **52**:17–33.
6. Carter BJ, Wawrzynek PA, Ingraffea AR. Automated 3D crack growth simulation. *International Journal for Numerical Methods in Engineering* 2000; **47**:229–253.
7. Belytschko T, Lu YY, Gu L, Tabbara M. Element-free Galerkin methods for static and dynamic fracture. *International Journal of Solids and Structures* 1994; **32**:2547–2570.
8. Belytschko T, Black T. Elastic crack growth in finite elements with minimal remeshing. *International Journal for Numerical Methods in Engineering* 1999; **45**:601–620.
9. Moës N, Dolbow J, Belytschko T. A finite element method for crack growth without remeshing. *International Journal for Numerical Methods in Engineering* 1999; **46**:131–150.
10. Johnson KL, Shercliff HR. Shakedown of 2-dimensional asperities in sliding contact. *International Journal of Mechanical Sciences* 1992; **34**:375–394.
11. Man KW, Aliabadi MH, Rooke DP. BEM frictional contact analysis: load incremental technique. *Computers and Structures* 1993; **47**:893–905.
12. Huesmann A, Kuhn G. Automatic load incrementation technique for plane elastoplastic frictional contact problems using boundary element method. *Computers and Structures* 1995; **56**:733–744.
13. Ingraffea AR, Heuze FE. Finite element models for rock fracture mechanics. *International Journal for Numerical and Analytical Methods in Geomechanics* 1980; **4**:25–43.
14. Zang WL, Gudmundson P. Contact problems of kinked cracks modelled by a boundary integral method. *International Journal for Numerical Methods in Engineering* 1990; **29**:847–860.
15. Zang WL, Gudmundson P. Frictional contact problems of kinked cracks modelled by a boundary integral method. *International Journal for Numerical Methods in Engineering* 1991; **31**:427–446.
16. Chen T-C, Chen W-H. Frictional contact analysis of multiple cracks by incremental displacement and resultant traction boundary integral equations. *Engineering Analysis with Boundary Elements* 1998; **21**:339–348.
17. Liu SB, Tan CL. Two-dimensional boundary element contact mechanics analysis of angled crack problems. *Engineering Fracture Mechanics* 1992; **42**:273–288.

18. Lee SS. Analysis of crack closure problem using the dual boundary element method. *International Journal of Fracture* 1996; **77**:323–336.
19. Chan HCM, Li V, Einstein HH. A hybridized displacement discontinuity and indirect boundary element method to model fracture propagation. *International Journal of Fracture* 1990; **45**:263–282.
20. Shen B, Stephansson O. Modification of the G-criterion for crack propagation subjected to compression. *Engineering Fracture Mechanics* 1994; **47**:177–189.
21. Napier JAL, Malan DF. A viscoplastic discontinuum model of time-dependent fracture and seismicity in brittle rock. *International Journal of Rock Mechanics and Mining Sciences* 1997; **34**:1075–1089.
22. Bobet A, Einstein HH. Numerical modeling of fracture coalescence in a model rock material. *International Journal of Fracture* 1998; **92**:221–252.
23. Sirtori S. General stress analysis method by means of integral equations and boundary elements. *Meccanica* 1979; **14**:210–218.
24. Bonnet M, Maier G, Polizzotto C. Symmetric Galerkin boundary-element method. *Applied Mechanics Reviews* (ASME) 1998; **51**:669–704.
25. Bonnet M. *Boundary Integral Equation Methods for Solids and Fluids*. Wiley: England, 1995.
26. Maier G, Novati G, Cen Z. Symmetric-Galerkin boundary element method for quasi-brittle fracture and frictional contact problems. *Computational Mechanics* 1995; **17**:74–89.
27. Crouch SL. Solution of plane elasticity problems by the displacement discontinuity method. *International Journal for Numerical Methods in Engineering* 1976; **10**:301–343.
28. Bui HD. An integral equation method for solving the problem of a plane crack of arbitrary shape. *Journal of the Mechanics and Physics of Solids* 1977; **25**:29–39.
29. Li S, Mear ME, Xiao L. Symmetric weak form integral equation method for three-dimensional fracture analysis. *Computer Methods in Applied Mechanics and Engineering* 1998; **151**:435–459.
30. Gray LJ, Griffith B. A faster Galerkin boundary integral algorithm. *Communications in Numerical Methods in Engineering* 1998; **14**:1109–1117.
31. Gray LJ. Evaluation of hypersingular integrals in the boundary element method. *Mathematical and Computer Modelling* 1991; **15**:165–174.
32. Martin PA, Rizzo FJ. Hypersingular integrals: how smooth must the density be? *International Journal for Numerical Methods in Engineering* 1996; **39**:687–704.
33. Rizzo FJ. An integral equation approach to boundary value problems of classical elastostatics. *Quarterly of Applied Mathematics* 1967; **25**:83–95.
34. Henshell RD, Shaw KG. Crack tip finite elements are unnecessary. *International Journal for Numerical Methods in Engineering* 1975; **9**:495–507.
35. Barsoum RS. On the use of isoparametric finite elements in linear fracture mechanics. *International Journal for Numerical Methods in Engineering* 1976; **10**:25–37.
36. Gray LJ, Phan A-V, Paulino GH, Kaplan T. Improved quarter-point crack tip element. *Engineering Fracture Mechanics* 2003; **70**:269–283.
37. Brebbia CA. *The Boundary Element Method for Engineers*. Wiley: New York, 1978.

